
SLAPS: Self-Supervision Improves Structure Learning for Graph Neural Networks

Bahare Fatemi*

University of British Columbia
bfatemi@cs.ubc.ca

Layla El Asri
Borealis AI

layla.elasri@borealisai.com

Seyed Mehran Kazemi*
Google Research

mehrankazemi@google.com

Abstract

Graph neural networks (GNNs) work well when the graph structure is provided. However, this structure may not always be available in real-world applications. One solution to this problem is to infer a task-specific latent structure and then apply a GNN to the inferred graph. Unfortunately, the space of possible graph structures grows super-exponentially with the number of nodes and so the task-specific supervision may be insufficient for learning both the structure and the GNN parameters. In this work, we propose the **Simultaneous Learning of Adjacency and GNN Parameters with Self-supervision**, or SLAPS, a method that provides more supervision for inferring a graph structure through self-supervision. A comprehensive experimental study demonstrates that SLAPS scales to large graphs with hundreds of thousands of nodes and outperforms several models that have been proposed to learn a task-specific graph structure on established benchmarks.

1 Introduction

Graph representation learning has grown rapidly and found applications in domains where a natural graph of the data points is available [4, 26]. Graph neural networks (GNNs) [45] have been a key component to the success of the research in this area. Specifically, GNNs have shown promising results for semi-supervised classification when the available graph structure exhibits a high degree of homophily (i.e. connected nodes often belong to the same class) [63].

We study the applicability of GNNs to (semi-supervised) classification problems where a graph structure is *not* readily available. The existing approaches for this problem either fix a similarity graph between the nodes or learn the GNN parameters and a graph structure simultaneously (see Related Work). In both cases, one main goal is to construct or learn a graph structure with a high degree of homophily with respect to the labels to aid the GNN classification. The latter approach is sometimes called *latent graph learning* and often results in higher predictive performance compared to the former approach (see, e.g., [13]).

We identify a supervision starvation problem in latent graph learning approaches in which the edges between pairs of nodes that are far from labeled nodes receive insufficient supervision; this results in learning poor structures away from labeled nodes and hence poor generalization. We propose a solution for this problem by adopting a multi-task learning framework in which we supplement the classification task with a self-supervised task. The self-supervised task is based on the hypothesis

*Work was done when authors were at Borealis AI.

that a graph structure that is suitable for predicting the node features is also suitable for predicting the node labels. It works by masking some input features (or adding noise to them) and training a separate GNN aiming at updating the adjacency matrix in such a way that it can recover the masked (or noisy) features. The task is generic and can be combined with several existing latent graph learning approaches.

We develop a latent graph learning model, dubbed SLAPS, that adopts the proposed self-supervised task. We provide a comprehensive experimental study on nine datasets (thirteen variations) of various sizes and from various domains and perform thorough analyses to show the merit of SLAPS.

Our main contributions include: 1) identifying a supervision starvation problem for latent graph learning, 2) proposing a solution for the identified problem through self-supervision, 3) developing SLAPS, a latent graph learning model that adopts the self-supervised solution, 4) providing comprehensive experimental results showing SLAPS substantially outperforms existing latent graph learning baselines from various categories on various benchmarks, and 5) providing an implementation for latent graph learning that scales to graphs with hundreds of thousands of nodes.

2 Related work

Existing methods that relate to this work can be grouped into the following categories. We discuss selected work from each category and refer the reader to [67] for a full survey.

Similarity graph: One approach for inferring a graph structure is to select a similarity metric and set the edge weight between two nodes to be their similarity [44, 49, 3]. To obtain a sparse structure, one may create a kNN similarity graph, only connect pairs of nodes whose similarity surpasses some predefined threshold, or do sampling. As an example, in [15] a (fixed) kNN graph using the cosine similarity of the node features is created. In [53], this idea is extended by creating a fresh graph in each layer of the GNN based on the node embedding similarities in that layer. Instead of choosing a single similarity metric, in [16] several (potentially weak) measures of similarity are fused. The quality of the predictions of these methods depends heavily on the choice of the similarity metric(s).

Fully connected graph: Another approach is to start with a fully connected graph and assign edge weights using the available meta-data or employ the GNN variants that provide weights for each edge via an attention mechanism [50, 59]. This approach has been used in computer vision [e.g., 48], natural language processing [e.g., 62], and few-shot learning [e.g., 14]. The complexity of this approach grows rapidly making it applicable only to small-sized graphs. Zhang et al. [60] propose to define local neighborhoods for each node and only assume that these local neighborhoods are fully connected. Their approach relies on an initial graph structure to define the local neighborhoods.

Latent graph learning: Instead of a similarity graph based on the initial features, one may use a graph generator with learnable parameters. In [34], a fully connected graph is created based on a bilinear similarity function with learnable parameters. In [13], a Bernoulli distribution is learned for each possible edge and graph structures are created through sampling from these distributions. In [55], the input structure is updated to increase homophily based on the labels and model predictions. In [6], an iterative approach is proposed that iterates over projecting the nodes to a latent space and constructing an adjacency matrix from the latent representations multiple times. A common approach in this category is to learn a projection of the nodes to a latent space where node similarities correspond to edge weights or edge probabilities. In [54], the nodes are projected to a latent space by learning weights for each of the input features. In [43, 22, 9], a multi-layer perceptron is used for projection. In [58, 61], a GNN is used for projection; it uses the node features and an initial graph structure. In [27], different graph structures are created in different layers by using separate GNN projectors, where the input to the GNN projector in a layer is the projected values and the generated graph structure from the previous layer. In our experiments, we compare with several approaches from this category.

Leveraging domain knowledge: In some applications, one may leverage domain knowledge to guide the model toward learning specific structures. For example, in [25], abstract syntax trees and regular languages are leveraged in learning graph structures of Python programs that aid reasoning for downstream tasks. In [24], the structure learning is guided for robustness to adversarial attacks through the domain knowledge that clean adjacency matrices are often sparse and low-rank and exhibit feature smoothness along the connected nodes. Other examples in this category include

[20, 43]. In our paper, we experiment with general-purpose datasets without access to domain knowledge.

Proposed method: Our model falls within the latent graph learning category. We supplement the training with a self-supervised objective to increase the amount of supervision in learning a structure. Our self-supervised task is inspired by, and similar to, the pre-training strategies for GNNs [18, 19, 23, 57, 64] (specifically, we adopt the multi-task learning framework of You et al. [57]), but it differs from this line of work as we use self-supervision for learning a graph structure whereas the above methods use it to learn better (and, in some cases, transferable) GNN parameters.

3 Background and notation

We use lowercase letters to denote scalars, bold lowercase letters to denote vectors and bold uppercase letters to denote matrices. \mathbf{I} represents an identity matrix. For a vector \mathbf{v} , we represent its i^{th} element as v_i . For a matrix \mathbf{M} , we represent the i^{th} row as \mathbf{M}_i and the element at the i^{th} row and j^{th} column as \mathbf{M}_{ij} . For an attributed graph, we use n , m and f to represent the number of nodes, edges, and features respectively, and denote the graph as $\mathcal{G} = \{\mathcal{V}, \mathbf{A}, \mathbf{X}\}$ where $\mathcal{V} = \{v_1, \dots, v_n\}$ is a set of nodes, $\mathbf{A} \in \mathbb{R}^{n \times n}$ is an adjacency matrix with \mathbf{A}_{ij} indicating the weight of the edge from v_i to v_j ($\mathbf{A}_{ij} = 0$ implies no edge), and $\mathbf{X} \in \mathbb{R}^{n \times f}$ is a matrix whose rows correspond to node features.

Graph convolutional networks (GCNs) [29] are a powerful variant of GNNs. For a graph $\mathcal{G} = \{\mathcal{V}, \mathbf{A}, \mathbf{X}\}$ with a degree matrix \mathbf{D} , layer l of the GCN architecture can be defined as $\mathbf{H}^{(l)} = \sigma(\hat{\mathbf{A}}\mathbf{H}^{(l-1)}\mathbf{W}^{(l)})$ where $\hat{\mathbf{A}}$ represents a normalized adjacency matrix, $\mathbf{H}^{(l-1)} \in \mathbb{R}^{n \times d_{l-1}}$ represents the node representations in layer $l-1$ ($\mathbf{H}^{(0)} = \mathbf{X}$), $\mathbf{W}^{(l)} \in \mathbb{R}^{d_{l-1} \times d_l}$ is a weight matrix, σ is an activation function such as ReLU [38], and $\mathbf{H}^{(l)} \in \mathbb{R}^{n \times d_l}$ is the updated node embeddings. For undirected graphs where the adjacency is symmetric, $\hat{\mathbf{A}} = \mathbf{D}^{-\frac{1}{2}}(\mathbf{A} + \mathbf{I})\mathbf{D}^{-\frac{1}{2}}$ corresponds to a row-and-column normalized adjacency with self-loops, and for directed graphs where the adjacency is not necessarily symmetric, $\hat{\mathbf{A}} = \mathbf{D}^{-1}(\mathbf{A} + \mathbf{I})$ corresponds to a row normalized adjacency matrix with self-loops. Here, \mathbf{D} is a (diagonal) degree matrix for $(\mathbf{A} + \mathbf{I})$ defined as $\mathbf{D}_{ii} = 1 + \sum_j \mathbf{A}_{ij}$.

4 Proposed method: SLAPS

SLAPS consists of four components: 1) generator, 2) adjacency processor, 3) classifier, and 4) self-supervision. Figure 1 illustrates these components. In the next three subsections, we explain the first three components. Then, we point out a supervision starvation problem for a model based only on these components. Then we describe the self-supervision component as a solution to the supervision starvation problem and the full SLAPS model.

4.1 Generator

The generator is a function $G : \mathbb{R}^{n \times f} \rightarrow \mathbb{R}^{n \times n}$ with parameters θ_G which takes the node features $\mathbf{X} \in \mathbb{R}^{n \times f}$ as input and produces a matrix $\tilde{\mathbf{A}} \in \mathbb{R}^{n \times n}$ as output. We consider the following two generators and leave experimenting with more sophisticated graph generators (e.g., [56, 36, 35]) and models with tractable adjacency computations (e.g., [7]) as future work.

Full parameterization (FP): For this generator, $\theta_G \in \mathbb{R}^{n \times n}$ and the generator function is defined as $\tilde{\mathbf{A}} = G_{FP}(\mathbf{X}; \theta_G) = \theta_G$. That is, the generator ignores the input node features and directly optimizes the adjacency matrix. FP is similar to the generator in [13] except that they treat each element of $\tilde{\mathbf{A}}$ as the parameter of a Bernoulli distribution and sample graph structures from these distributions. FP is simple and flexible for learning any adjacency matrix but adds n^2 parameters which limits scalability and makes the model susceptible to overfitting.

MLP-kNN: Here, θ_G corresponds to the weights of a multi-layer perceptron (MLP) and $\tilde{\mathbf{A}} = G_{MLP}(\mathbf{X}; \theta_G) = \text{kNN}(\text{MLP}(\mathbf{X}))$, where $\text{MLP} : \mathbb{R}^{n \times f} \rightarrow \mathbb{R}^{n \times f'}$ is an MLP that produces a matrix with updated node representations \mathbf{X}' ; $\text{kNN} : \mathbb{R}^{n \times f'} \rightarrow \mathbb{R}^{n \times n}$ produces a sparse matrix. The implementation details for the kNN operation is provided in the supplementary material.

Initialization and variants of MLP-kNN: Let \mathbf{A}^{kNN} represent an adjacency matrix created by applying a kNN function on the initial node features. One smart initialization for θ_G is to initialize it

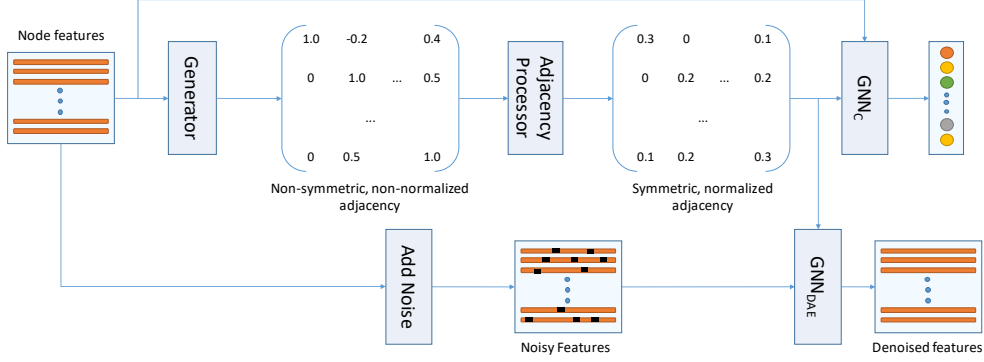


Figure 1: Overview of SLAPS. At the top, a generator receives the node features and produces a non-symmetric, non-normalized adjacency having (possibly) both positive and negative values (Section 4.1). The adjacency processor makes the values positive, symmetrizes and normalizes the adjacency (Section 4.2). The resulting adjacency and the node features go into GNN_C which predicts the node classes (Section 4.3). At the bottom, some noise is added to the node features. The resulting noisy features and the generated adjacency go into GNN_{DAE} which then denoises the features (Section 4.5).

in a way that the generator initially generates \mathbf{A}^{kNN} (i.e. $\tilde{\mathbf{A}} = \mathbf{A}^{kNN}$ before training starts). This can be trivially done for the FP generator by initializing θ_G to \mathbf{A}^{kNN} . For MLP-kNN, we consider two variants. In one, hereafter referred to simply as MLP, we keep the input dimension the same throughout the layers. In the other, hereafter referred to as MLP-D, we consider MLPs with diagonal weight matrices (i.e., except the main diagonal, all other parameters in the weight matrices are zero). For both variants, we initialize the weight matrices in θ_G with the identity matrix to ensure that the output of the MLP is initially the same as its input and the kNN graph created on these outputs is equivalent to \mathbf{A}^{kNN} (Alternatively, one may use other MLP variants but pre-train the weights to output \mathbf{A}^{kNN} before the main training starts.). MLP-D can be thought of as assigning different weights to different features and then computing node similarities.

4.2 Adjacency processor

The output $\tilde{\mathbf{A}}$ of the generator may have both positive and negative values, may be non-symmetric and non-normalized. We let $\mathbf{A} = \frac{1}{2} \mathbf{D}^{-\frac{1}{2}} (\mathbf{P}(\tilde{\mathbf{A}}) + \mathbf{P}(\tilde{\mathbf{A}})^T) \mathbf{D}^{-\frac{1}{2}}$. Here \mathbf{P} is a function with a non-negative range applied element-wise on its input – see supplementary material for details. The sub-expression $\frac{1}{2} (\mathbf{P}(\tilde{\mathbf{A}}) + \mathbf{P}(\tilde{\mathbf{A}})^T)$ makes the resulting matrix $\mathbf{P}(\tilde{\mathbf{A}})$ symmetric. To understand the reason for taking the mean of $\mathbf{P}(\tilde{\mathbf{A}})$ and $\mathbf{P}(\tilde{\mathbf{A}})^T$, assume $\tilde{\mathbf{A}}$ is generated by G_{MLP} . If v_j is among the k most similar nodes to v_i and vice versa, then the strength of the connection between v_i and v_j will remain the same. However, if, say, v_j is among the k most similar nodes to v_i but v_i is not among the top k for v_j , then taking the average of the similarities reduces the strength of the connection between v_i and v_j . Finally, once we have a symmetric adjacency with non-negative values, we normalize $\frac{1}{2} (\mathbf{P}(\tilde{\mathbf{A}}) + \mathbf{P}(\tilde{\mathbf{A}})^T)$ by computing its degree matrix \mathbf{D} and multiplying it from left and right to $\mathbf{D}^{-\frac{1}{2}}$.

4.3 Classifier

The classifier is a function $\text{GNN}_C : \mathbb{R}^{n \times f} \times \mathbb{R}^{n \times n} \rightarrow \mathbb{R}^{n \times |\mathcal{C}|}$ with parameters θ_{GNN_C} . It takes the node features \mathbf{X} and the generated adjacency \mathbf{A} as input and provides for each node the logits for each class. \mathcal{C} corresponds to the classes and $|\mathcal{C}|$ corresponds to the number of classes. We use a two-layer GCN for which $\theta_{\text{GNN}_C} = \{\mathbf{W}^{(1)}, \mathbf{W}^{(2)}\}$ and define our classifier as $\text{GNN}_C(\mathbf{A}, \mathbf{X}; \theta_{\text{GNN}_C}) = \text{AReLU}(\mathbf{A}\mathbf{X}\mathbf{W}^{(1)})\mathbf{W}^{(2)}$ but other GNN variants can be used as well (recall that \mathbf{A} is normalized). The training loss \mathcal{L}_C for the classification task is computed by taking the softmax of the logits to produce a probability distribution for each node and then computing the cross-entropy loss.

4.4 Using only the first three components leads to supervision starvation

One may create a model using only the three components described so far corresponding to the top part of Figure 1. As we will explain here, however, this model may suffer severely from supervision starvation. The same problem also applies to many existing approaches for latent graph learning, as they can be formulated as a combination of variants of these three components.

Consider a scenario during training where two unlabeled nodes v_i and v_j are not directly connected to any labeled nodes according to the generated structure. Then, since a two-layer GCN makes predictions for the nodes based on their two-hop neighbors, the classification loss (i.e. \mathcal{L}_C) is not affected by the edge between v_i and v_j and this edge receives no supervision². Figure 2 provides an example of such a scenario. Let us call the edges that do not affect the loss function \mathcal{L}_C (and consequently do not receive supervision) as *starved edges*. These edges are problematic because although they may not affect the training loss, the predictions at the test time depend on these edges and if their values are learned without enough supervision, the model may make poor predictions at the test time. A natural question concerning the extent of the problem caused by such edges is the proportion of starved edges. The following theorem formally establishes the extent of the problem for Erdős-Rényi graphs [11]; in the supplementary, we extend this result to the Barabási-Albert model [1] and scale-free networks [2]. An *Erdős-Rényi* graph with n nodes and m edges is a graph chosen uniformly at random from the collection of all graphs which have n nodes and m edges.

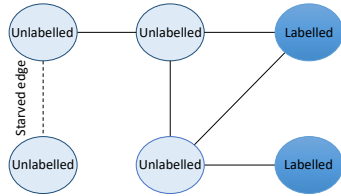


Figure 2: Using a two-layer GCN, the predictions made for the labeled nodes are not affected by the dashed (starved) edge.

Theorem 1 Let $\mathcal{G}(n, m)$ be an Erdős-Rényi graph with n nodes and m edges. Assume we have labels for q nodes selected uniformly at random. The probability of an edge being a starved edge with a two-layer GCN is equal to $(1 - \frac{q}{n})(1 - \frac{q}{n-1}) \prod_{i=1}^{2q} (1 - \frac{m-1}{\binom{n}{2}-i})$.

We defer the proof to the supplementary material. To put the numbers from the theorem in perspective, let us consider three established benchmarks for semi-supervised node classification namely *Cora*, *Citeseer*, and *Pubmed* (the statistics for these datasets can be found in the Appendix). For an Erdős-Rényi graph with similar statistics as the Cora dataset ($n = 2708$, $m = 5429$, $q = 140$), the probability of an edge being a starved edge is 59.4% according to the above theorem. For Citeseer and Pubmed, this number is 75.7% and 96.7% respectively. While Theorem 1 is stated for Erdős-Rényi graphs, the identified problem also applies to natural graphs. For the original structures of Cora, Citeseer, and Pubmed, for example, 48.8%, 65.2%, and 91.6% of the edges are starved edges.

4.5 Self-supervision

One possible solution to the supervision starvation problem is to define a *prior graph structure* and regularize the learned structure toward it. This leads the starved edges toward the prior structure as opposed to neglecting them. The choice of the prior is important as it determines the inductive bias incorporated into the model. We define a prior structure based on the following hypothesis:

Hypothesis 1 A graph structure that is suitable for predicting the node features is also suitable for predicting the node labels.

We first explain why the above hypothesis is reasonable for an extreme case that is easy to understand and then extend the explanation to the general case. Consider an extreme scenario where one of the node features is the same as the node labels. A graph structure that is suitable for predicting this feature exhibits homophily for it. Because of the equivalence between this feature and the labels, the graph structure also exhibits homophily for the labels, so it is also suitable for predicting the labels. In the general (non-extreme) case, there may not be a single feature that is equivalent to the labels but a subset of the features may be highly predictive of the labels. A graph structure that is suitable for predicting this subset exhibits homophily for the features in the subset. Because this subset is highly

²While using more layers may somewhat alleviate this problem, deeper GCNs typically produce inferior results, e.g., due to oversmoothing [33, 39] – see the supplementary material for empirical evidence.

predictive of the labels, the structure also exhibits a high degree of homophily for the labels, so it is also suitable for predicting the node labels.

Next, we explain how to design a suitable graph structure for predicting the features and how to regularize toward it. One could design such a structure manually (e.g., by handcrafting a graph that connects nodes based on the collective homophily between their individual features) and then penalize the difference between this prior graph and the learned graph. Alternatively, in this paper, we take a learning-based approach based on self-supervision where we not only use the learned graph structure for the classification task, but also for denoising the node features. The self-supervised task encourages the model to learn a structure that is suitable for predicting the node features. We describe this approach below and provide comparisons to the manual approach in the supplementary material.

Our self-supervised task is based on denoising autoencoders [51]. Let $\text{GNN}_{\text{DAE}} : \mathbb{R}^{n \times f} \times \mathbb{R}^{n \times n} \rightarrow \mathbb{R}^{n \times f}$ be a GNN with parameters $\theta_{\text{GNN}_{\text{DAE}}}$ that takes node features and a generated adjacency as input and provides updated node features with the same dimension as output. We train GNN_{DAE} such that it receives a noisy version $\tilde{\mathbf{X}}$ of the features \mathbf{X} as input and produces the denoised features \mathbf{X} as output. Let idx represent the indices corresponding to the elements of \mathbf{X} to which we have added noise, and \mathbf{X}_{idx} represent the values at these indices. During training, we minimize:

$$\mathcal{L}_{\text{DAE}} = \text{L}(\mathbf{X}_{idx}, \text{GNN}_{\text{DAE}}(\tilde{\mathbf{X}}, \mathbf{A}; \theta_{\text{GNN}_{\text{DAE}}})_{idx}) \quad (1)$$

where \mathbf{A} is the generated adjacency matrix and L is a loss function. For datasets where the features consist of binary vectors, idx consists of r percent of the indices of \mathbf{X} whose values are 1 and $r\eta$ percent of the indices whose values are 0, both selected uniformly at random in each epoch. Both r and η (corresponding to the negative ratio) are hyperparameters. In this case, we add noise by setting the 1s in the selected mask to 0s and L is the binary cross-entropy loss. For datasets where the input features are continuous numbers, idx consists of r percent of the indices of \mathbf{X} selected uniformly at random in each epoch. We add noise by either replacing the values at idx with 0 or by adding independent Gaussian noises to each of the features. In this case, L is the mean-squared error loss.

Note that the self-supervised task in equation 1 is generic and can be added to different GNNs as well as latent graph learning models. It can be also combined with other techniques in the literature that encourage learning more homophilous structures or increase the amount of supervision. In our experiments, we test the combination of our self-supervised task with two such techniques namely *self-training* [33] and *AdaEdge* [5]. *Self-training* helps the model “see” more labeled nodes and *AdaEdge* helps iteratively create graph structure with higher degrees of homophily. We refer the reader to the supplementary material for descriptions of *self-training* and *AdaEdge*.

4.6 SLAPS

Our final model is trained to minimize $\mathcal{L} = \mathcal{L}_C + \lambda \mathcal{L}_{\text{DAE}}$ where \mathcal{L}_C is the classification loss, \mathcal{L}_{DAE} is the denoising autoencoder loss (see Equation 1), and λ is a hyperparameter controlling the relative importance of the two losses.

5 Experiments

In this section, we report our key results. More empirical comparisons, experimental analyses, and ablation studies are presented in the supplementary material.

Baselines: We compare our proposal to several baselines with different properties. The first baseline is a multi-layer perceptron (MLP) which does not take the graph structure into account. We also compare against MLP-GAM* [47] which learns a fully connected graph structure and uses this structure to supplement the loss function of the MLP toward predicting similar labels for neighboring nodes. Our third baseline is label propagation (LP) [65], a well-known model for semi-supervised learning. Similar to [13], we also consider a baseline named *kNN-GCN* where we create a kNN graph based on the node feature similarities and feed this graph to a GCN; the graph structure remains fixed in this approach. We also compare with prominent existing latent graph learning models including LDS [13], GRCN [58], DGCNN [53], and IDGL [6]. In [6], another variant named IDGL-ANCH is also proposed that reduces time complexity through anchor-based approximation [37]. We compare against the base IDGL model because it does not sacrifice accuracy for time complexity, and because anchor-based approximation is model-agnostic and could be combined with other models too. We

Table 1: Results of SLAPS and the baselines on established node classification benchmarks. † indicates results have been taken from Franceschi et al. [13]. ‡ indicates results have been taken from Stretcu et al. [47]. Bold and underlined values indicate best and second-best mean performances respectively. *OOM* indicates out of memory. *OOT* indicates out of time (we allowed 24h for each run). *NA* indicates not applicable.

Model	Cora	Citeseer	Cora390	Citeseer370	Pubmed	ogbn-arxiv
MLP	56.1 ± 1.6 [†]	56.7 ± 1.7 [†]	65.8 ± 0.4	67.1 ± 0.5	71.4 ± 0.0	<u>54.7 ± 0.1</u>
MLP-GAM*	70.7 [‡]	70.3 [‡]	—	—	71.9 [‡]	—
LP	37.6 ± 0.0	23.2 ± 0.0	36.2 ± 0.0	29.1 ± 0.0	41.3 ± 0.0	OOM
kNN-GCN	66.5 ± 0.4 [†]	68.3 ± 1.3 [†]	72.5 ± 0.5	71.8 ± 0.8	70.4 ± 0.4	49.1 ± 0.3
LDS	—	—	71.5 ± 0.8 [†]	71.5 ± 1.1 [†]	OOM	OOM
GRCN	67.4 ± 0.3	67.3 ± 0.8	71.3 ± 0.9	70.9 ± 0.7	67.3 ± 0.3	OOM
DGCNN	56.5 ± 1.2	55.1 ± 1.4	67.3 ± 0.7	66.6 ± 0.8	70.1 ± 1.3	OOM
IDGL	70.9 ± 0.6	68.2 ± 0.6	73.4 ± 0.5	72.7 ± 0.4	72.3 ± 0.4	OOM
kNN-GCN + AdaEdge	67.7 ± 1.0	68.8 ± 1.0	72.2 ± 0.4	71.8 ± 0.6	OOT	OOT
kNN-GCN + self-training	67.3 ± 0.3	69.8 ± 1.0	71.1 ± 0.3	72.4 ± 0.2	72.7 ± 0.1	NA
SLAPS (FP)	72.4 ± 0.4	70.7 ± 0.4	76.6 ± 0.4	73.1 ± 0.6	OOM	OOM
SLAPS (MLP)	72.8 ± 0.8	70.5 ± 1.1	75.3 ± 1.0	73.0 ± 0.9	74.4 ± 0.6	56.6 ± 0.1
SLAPS (MLP-D)	73.4 ± 0.3	72.6 ± 0.6	75.1 ± 0.5	73.9 ± 0.4	73.1 ± 0.7	52.9 ± 0.1
SLAPS (MLP) + AdaEdge	72.8 ± 0.7	70.6 ± 1.5	75.2 ± 0.6	72.6 ± 1.4	OOT	OOT
SLAPS (MLP) + self-training	74.2 ± 0.5	73.1 ± 1.0	<u>75.5 ± 0.7</u>	<u>73.3 ± 0.6</u>	<u>74.3 ± 1.4</u>	NA

feed a kNN graph to the models requiring an initial graph structure. We also explore how adding self-training and AdaEdge impact the performance of kNN-GCN as well as SLAPS.

Datasets: We use three established benchmarks in the GNN literature namely Cora, Citeseer, and Pubmed [46] as well as the *ogbn-arxiv* dataset [17] that is orders of magnitude larger than the other three datasets and is more challenging due to the more realistic split of the data into train, validation, and test sets. For these datasets, we only feed the node features to the models and not their original graph structure. Following [13, 6], we also experiment with several classification (non-graph) datasets available in scikit-learn [41] including Wine, Cancer, Digits, and 20News. Furthermore, following [21], we also provide results on MNIST [31]. The dataset statistics can be found in the supplementary. For Cora and Citeseer, the LDS model uses the train data for learning the parameters of the classification GCN, half of the validation for learning the parameters of the adjacency matrix (in their bi-level optimization setup, these are considered as hyperparameters), and the other half of the validation set for early stopping and tuning the other hyperparameters. Besides experimenting with the original setups of these two datasets, we also consider a setup that is closer to that of LDS: we use the train set and half of the validation set for training and the other half of validation for early stopping and hyperparameter tuning. We name the modified versions Cora390 and Citeseer370 respectively where the number proceeding the dataset name shows the number of labels from which gradients are computed. We follow a similar procedure for the scikit-learn datasets.

Implementation: We defer the implementation details and the best hyperparameter settings for our model on all the datasets to the supplementary material. Code and data is available at <https://github.com/BorealisAI/SLAPS-GNN>.

5.1 Comparative results

The results of SLAPS and the baselines on our benchmarks are reported in Tables 1 and 2. We start by analyzing the results in Table 1 first. Starting with the baselines, we see that learning a fully connected graph in MLP-GAM* makes it outperform MLP. kNN-GCN significantly outperforms MLP on Cora and Citeseer but underperforms on Pubmed and ogbn-arxiv. Furthermore, both self-training and AdaEdge improve the performance of kNN-GCN. This shows the importance of the similarity metric and the graph structure that is fed into GCN; a low-quality structure can harm model performance. LDS outperforms MLP but the fully parameterized adjacency matrix of LDS results in memory issues for Pubmed and ogbn-arxiv. As for GRCN, it was shown in the original paper that GRCN can revise a good initial adjacency matrix and provide a substantial boost in performance. However, as evidenced by the results, if the initial graph structure is somewhat poor, GRCN’s performance becomes on par with kNN-GCN. IDGL is the best performing baseline.

Table 2: Results on classification datasets. † indicates results have been taken from Franceschi et al. [13]. Bold and underlined values indicate best and second-best mean performances respectively.

Model	Wine	Cancer	Digits	20news
MLP	96.1 ± 1.0	95.3 ± 0.9	81.9 ± 1.0	30.4 ± 0.1
kNN-GCN	93.5 ± 0.7	95.3 ± 0.4	95.4 ± 0.4	46.3 ± 0.3
LDS	97.3 ± 0.4 †	94.4 ± 1.9†	92.5 ± 0.7†	46.4 ± 1.6†
IDGL	97.0 ± 0.7	94.2 ± 2.3	92.5 ± 1.3	48.5 ± 0.6
SLAPS (FP)	96.6 ± 0.4	94.6 ± 0.3	94.4 ± 0.7	44.4 ± 0.8
SLAPS (MLP)	96.3 ± 1.0	96.0 ± 0.8	92.5 ± 0.7	50.4 ± 0.7
SLAPS (MLP-D)	96.5 ± 0.8	96.6 ± 0.2	94.2 ± 0.1	<u>49.8 ± 0.9</u>

In addition to the aforementioned baselines, we also experimented with GCN, GAT, and Transformer (encoder only) architectures applied on fully connected graphs. GCN always learned to predict the majority class. This is because after one fully connected GCN layer, all nodes will have the same embedding and become indistinguishable. GAT also showed similar behavior. We believe this is because the attention weights are (almost) random at the beginning (due to random initialization of the model parameters) resulting in nodes becoming indistinguishable and GAT cannot escape from that state. The skip connections of Transformer helped avoid the problem observed for GCN and GAT and we were able to achieve better results ($\sim 40\%$ accuracy on Cora). However, we observed severe overfitting (even with very small models and with high dropout probabilities).

SLAPS consistently outperforms the baselines in some cases by large margins. Among the generators, the winner is dataset-dependent with MLP-D mostly outperforming MLP on datasets with many features and MLP outperforming on datasets with small numbers of features. Using the software that was publicly released by the authors, the baselines that learn a graph structure fail on ogbn-arxiv³; our implementation, on the other hand, scales to such large graphs. Adding self-training helps further improve the results of SLAPS. Adding AdaEdge, however, does not seem effective, probably because the graph structure learned by SLAPS already exhibits a high degree of homophily (see Section 5.4).

In Table 2, we only compared SLAPS with the best performing baselines from Table 1 (kNN-GCN, LDS and IDGL). We also included an MLP baseline for comparison. On three out of four datasets, SLAPS outperforms the LDS and IDGL baselines. For the Digits dataset, interestingly kNN-GCN outperforms the learning-based models. This could be because the initial kNN structure for this dataset is already a good structure. Among the datasets on which we can train SLAPS with the FP generator, 20news has the largest number of nodes (9,607 nodes). On this dataset, we observed that an FP generator suffers from overfitting and produces weaker results compared to other generators due to its large number of parameters.

Jiang et al. [22] show that learning a latent graph structure of the input examples can help with semi-supervised image classification. In particular, they create three versions of the MNIST dataset each consisting of a randomly selected subset with 10,000 examples in total. The first version contains 1000 labels for training, the second contains 2000, and the third version contains 3000 labels for training. All three variants use an extra 1000 labels for validation. The other examples are used as test examples. Here, we conduct an experiment to measure the performance of SLAPS on these variants of the MNIST dataset. We compare against GLCN [22] as well as the baselines in the GLCN paper including manifold regularization [3], label propagation, deep walk [42], graph convolutional networks (GCN), and graph attention networks (GAT).

Table 3: Results on the MNIST dataset. Bold values indicate best mean performances. Underlined values indicate second best mean performance. All the results for baseline have been taken from [21].

Model	MNIST1000	MNIST2000	MNIST3000
ManiReg	92.74 ± 0.3	93.96 ± 0.2	94.62 ± 0.2
LP	79.28 ± 0.9	81.91 ± 0.8	83.45 ± 0.5
DeepWalk	94.55 ± 0.3	95.04 ± 0.3	95.34 ± 0.3
GCN	90.59 ± 0.3	90.91 ± 0.2	91.01 ± 0.2
GAT	92.11 ± 0.4	92.64 ± 0.3	92.81 ± 0.3
GLCN	94.28 ± 0.3	95.09 ± 0.2	<u>95.46 ± 0.2</u>
SLAPS	94.66 ± 0.2	95.35 ± 0.1	95.54 ± 0.0

The results are reported in Table 3. From the results, it can be viewed that SLAPS outperforms GLCN and all the other baselines on the 3 variants. Compared to GLCN, on the three variants SLAPS

³We note that IDGL-ANCH also scales to ogbn-arxiv.

reduces the error by 7%, 5%, and 2% respectively, showing that SLAPS can be more effective when the labeled set is small and providing more empirical evidence for Theorem 1.

5.2 The effectiveness of self-supervision

Learning a structure only using self-supervision: To provide more insight into the value provided by the self-supervision task and the generalizability of the adjacency learned through this task, we conduct experiments with a variant of SLAPS named $SLAPS_{2s}$ that is trained in two stages. We first train the GNN_{DAE} model by minimizing \mathcal{L}_{DAE} described in in Equation 1. Recall that \mathcal{L}_{DAE} depends on the parameters θ_G of the generator and the parameters $\theta_{GNN_{DAE}}$ of the denoising autoencoder. After every t epochs of training, we fix the adjacency matrix, train a classifier with the fixed adjacency matrix, and measure classification accuracy on the validation set. We select the epoch that produces the adjacency providing the best validation accuracy for the classifier. Note that in $SLAPS_{2s}$, the adjacency matrix only receives gradients from the self-supervised task in Equation 1.

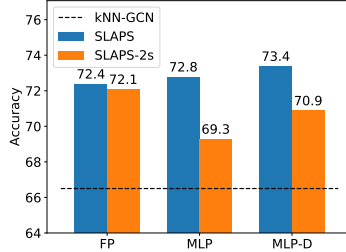


Figure 3: SLAPS vs SLAPS_{2s} on Cora with different generators.

Figure 3 shows the performance of SLAPS and SLAPS_{2s} on Cora and compares them with kNN-GCN. Although SLAPS_{2s} does not use the node labels in learning an adjacency matrix, it outperforms kNN-GCN (8.4% improvement when using an FP generator). With an FP generator, SLAPS_{2s} even achieves competitive performance with SLAPS; this is mainly because FP does not leverage the supervision provided by GCN_C toward learning generalizable patterns that can be used for nodes other than those in the training set. These results corroborate the effectiveness of the self-supervision task for learning an adjacency matrix. Besides, the results show that learning the adjacency using both self-supervision and the task-specific node labels results in higher predictive accuracy.

The value of λ : Figure 4 shows the performance of SLAPS⁴ on Cora and Citeseer with different values of λ . When $\lambda = 0$, corresponding to removing self-supervision, the model performance is somewhat poor. As soon as λ becomes positive, both models see a large boost in performance showing that self-supervision is crucial to the high performance of SLAPS. Increasing λ further provides larger boosts until it becomes so large that the self-supervision loss dominates the classification loss and the performance deteriorates. Note that with $\lambda = 0$, SLAPS with the MLP generator becomes a variant of the model proposed in [9], but with a different similarity function.

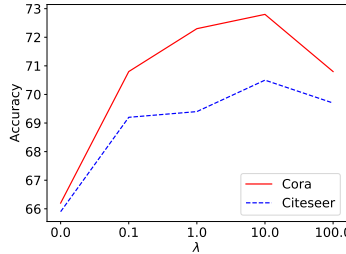


Figure 4: The performance of SLAPS with MLP graph generator as a function of λ .

Is self-supervision actually solving the supervision starvation problem? In Fig 4, we showed that self-supervision is key to the high performance of SLAPS. Here, we examine if this is because self-supervision indeed addresses the supervision starvation problem. For this purpose, we compared SLAPS

with and without self-supervision on two groups of test nodes on Cora: 1) those that are not connected to any labeled nodes after training, and 2) those that are connected to at least one labeled node after training. The nodes in group one have a high chance of having starved edges. We observed that adding self-supervision provides 38.0% improvement for the first group and only 8.9% improvement for the latter. Since self-supervision mainly helps with nodes in group 1, this provides evidence that self-supervision is an effective solution to the supervision starvation problem.

The effect of the training set size: According to Theorem 1, a smaller q (corresponding to the training set size) results in more starved edges in each epoch. To explore the effect of self-supervision as a function of q , we compared SLAPS with and without supervision on Cora and Citeseer while reducing the number of labeled nodes per class from 20 to 5. We used the FP generator for this experiment. With 5 labeled nodes per class, adding self-supervision provides 16.7% and 22.0%

⁴The generator used in this experiment is MLP; other generators produced similar results.

improvements on Cora and Citeseer respectively, which is substantially higher than the corresponding numbers when using 20 labeled nodes per class (10.0% and 7.0% respectively). This provides empirical evidence for Theorem 1. Note that the results on Cora390 and Citeseer 370 datasets provide evidence that the self-supervised task is effective even when the label rate is high.

5.3 Experiments with noisy graphs

The performance of GNNs highly depends on the quality of the input graph structure and deteriorates when the graph structure is noisy [see 68, 10, 12]. Here, we verify whether self-supervision is also helpful when a noisy structure is provided as input. Toward this goal, we experiment with Cora and Citeseer and provide noisy versions of the input graph as input. The provided noisy graph structure is used only for initialization; it is then further optimized by SLAPS. We perturb the graph structure by replacing ρ percent of the edges in the original structure (selected uniformly at random) with random edges. Figure 5 shows the performance of SLAPS with and without self-supervision ($\lambda = 0$ corresponds to no supervision). We also report the results of vanilla GCN on these perturbed graphs for comparison. It can be viewed that self-supervision consistently provides a boost in performance especially for higher values of ρ .

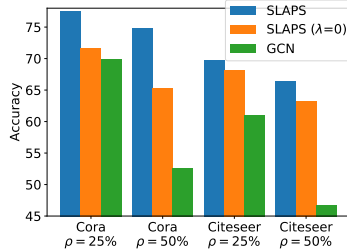


Figure 5: Performance comparison when noisy graphs are provided as input (ρ indicates the percentage of perturbations).

5.4 Analyses of the learned adjacency

Noisy graphs: Following the experiment in Section 5.3, we compared the learned and original structures by measuring the number of random edges added during perturbation but removed by the model and the number of edges removed during the perturbation but recovered by the model. For Cora, SLAPS removed 76.2% and 70.4% of the noisy edges and recovered 58.3% and 44.5% of the removed edges for $\rho = 25\%$ and $\rho = 50\%$ respectively while SLAPS with $\lambda = 0$ only removed 62.8% and 54.9% of the noisy edges and recovered 51.4% and 35.8% of the removed edges. This provides evidence on self-supervision being helpful for structure learning.

Homophily: As explained earlier, a properly learned graph for semi-supervised classification with GNNs exhibits high homophily. To verify the quality of the learned adjacency with respect to homophily, for every pair of nodes in the test set, we compute the odds of the two nodes sharing the same label as a function of the normalized weight of the edge connecting them. Figure 6 represents the odds for different weight intervals (recall that \mathbf{A} is row and column normalized). For both Cora and Citeseer, nodes' connected with higher edge weights are more likely to share the same label compared to nodes with lower or zero edge weights. Specifically, when $A_{ij} \geq 0.1$, v_i and v_j are almost 2.5 and 2.0 times more likely to share the same label on Cora and Citeseer respectively.

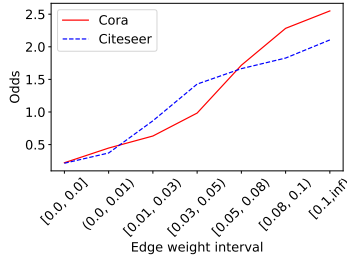


Figure 6: The odds of two nodes in the test set sharing the same label as a function of the edge weights learned by SLAPS.

6 Conclusion

We proposed SLAPS: a model for learning the parameters of a graph neural network and a graph structure of the nodes connectivities simultaneously from data. We identified a supervision starvation problem that emerges for graph structure learning, especially when training data is scarce. We proposed a solution to the supervision starvation problem by supplementing the training objective with a well-motivated self-supervised task. We showed the effectiveness of our model through a comprehensive set of experiments and analyses.

7 Funding Transparency Statement

This work was fully funded by Borealis AI.

References

- [1] Réka Albert and Albert-László Barabási. Statistical mechanics of complex networks. *Reviews of modern physics*, 74(1):47, 2002.
- [2] Albert-László Barabási and Réka Albert. Emergence of scaling in random networks. *science*, 286(5439):509–512, 1999.
- [3] Mikhail Belkin, Partha Niyogi, and Vikas Sindhwani. Manifold regularization: A geometric framework for learning from labeled and unlabeled examples. *JMLRR*, 7(Nov):2399–2434, 2006.
- [4] Ines Chami, Sami Abu-El-Haija, Bryan Perozzi, Christopher Ré, and Kevin Murphy. Machine learning on graphs: A model and comprehensive taxonomy. *arXiv preprint arXiv:2005.03675*, 2020.
- [5] Deli Chen, Yankai Lin, Wei Li, Peng Li, Jie Zhou, and Xu Sun. Measuring and relieving the over-smoothing problem for graph neural networks from the topological view. In *Proceedings of the AAAI Conference on Artificial Intelligence*, volume 34, pages 3438–3445, 2020.
- [6] Yu Chen, Lingfei Wu, and Mohammed J. Zaki. Deep iterative and adaptive learning for graph neural networks. In *Neural Information Processing Systems (NeurIPS)*, 2020.
- [7] Krzysztof Choromanski, Valerii Likhoshesterov, David Dohan, Xingyou Song, Andreea Gane, Tamas Sarlos, Peter Hawkins, Jared Davis, Afroz Mohiuddin, Lukasz Kaiser, et al. Rethinking attention with performers. *arXiv preprint arXiv:2009.14794*, 2020.
- [8] Djork-Arné Clevert, Thomas Unterthiner, and Sepp Hochreiter. Fast and accurate deep network learning by exponential linear units (elus). *arXiv preprint arXiv:1511.07289*, 2015.
- [9] Luca Cosmo, Anees Kazi, Seyed-Ahmad Ahmadi, Nassir Navab, and Michael Bronstein. Latent patient network learning for automatic diagnosis. *arXiv preprint arXiv:2003.13620*, 2020.
- [10] Hanjun Dai, Hui Li, Tian Tian, Xin Huang, Lin Wang, Jun Zhu, and Le Song. Adversarial attack on graph structured data. *arXiv preprint arXiv:1806.02371*, 2018.
- [11] Paul Erdős and Alfred Rényi. On random graphs. *Publicationes Mathematicae Debrecen*, 6: 290–297, 1959.
- [12] James Fox and Sivasankaran Rajamanickam. How robust are graph neural networks to structural noise? *arXiv preprint arXiv:1912.10206*, 2019.
- [13] Luca Franceschi, Mathias Niepert, Massimiliano Pontil, and Xiao He. Learning discrete structures for graph neural networks. In *ICML*, 2019.
- [14] Victor Garcia and Joan Bruna. Few-shot learning with graph neural networks. *arXiv preprint arXiv:1711.04043*, 2017.
- [15] Spyros Gidaris and Nikos Komodakis. Generating classification weights with gnn denoising autoencoders for few-shot learning. In *Proceedings of the IEEE Conference on Computer Vision and Pattern Recognition*, pages 21–30, 2019.
- [16] Jonathan Halcrow, Alexandru Mosoi, Sam Ruth, and Bryan Perozzi. Grale: Designing networks for graph learning. In *Proceedings of the 26th ACM SIGKDD International Conference on Knowledge Discovery & Data Mining*, pages 2523–2532, 2020.
- [17] Weihua Hu, Matthias Fey, Marinka Zitnik, Yuxiao Dong, Hongyu Ren, Bowen Liu, Michele Catasta, and Jure Leskovec. Open graph benchmark: Datasets for machine learning on graphs. *arXiv preprint arXiv:2005.00687*, 2020.

- [18] Weihua Hu, Bowen Liu, Joseph Gomes, Marinka Zitnik, Percy Liang, Vijay Pande, and Jure Leskovec. Strategies for pre-training graph neural networks. In *ICLR*, 2020.
- [19] Ziniu Hu, Yuxiao Dong, Kuansan Wang, Kai-Wei Chang, and Yizhou Sun. Gpt-gnn: Generative pre-training of graph neural networks. In *Proceedings of the 26th ACM SIGKDD International Conference on Knowledge Discovery & Data Mining*, pages 1857–1867, 2020.
- [20] Soobeom Jang, Seong-Eun Moon, and Jong-Seok Lee. Brain signal classification via learning connectivity structure. *arXiv preprint arXiv:1905.11678*, 2019.
- [21] Bo Jiang, Ziyang Zhang, Doudou Lin, Jin Tang, and Bin Luo. Semi-supervised learning with graph learning-convolutional networks. In *Proceedings of the IEEE/CVF Conference on Computer Vision and Pattern Recognition*, pages 11313–11320, 2019.
- [22] Bo Jiang, Ziyang Zhang, Doudou Lin, Jin Tang, and Bin Luo. Semi-supervised learning with graph learning-convolutional networks. In *Proceedings of the IEEE/CVF Conference on Computer Vision and Pattern Recognition*, pages 11313–11320, 2019.
- [23] Wei Jin, Tyler Derr, Haochen Liu, Yiqi Wang, Suhang Wang, Zitao Liu, and Jiliang Tang. Self-supervised learning on graphs: Deep insights and new direction. *arXiv preprint arXiv:2006.10141*, 2020.
- [24] Wei Jin, Yao Ma, Xiaorui Liu, Xianfeng Tang, Suhang Wang, and Jiliang Tang. Graph structure learning for robust graph neural networks. *arXiv preprint arXiv:2005.10203*, 2020.
- [25] Daniel D Johnson, Hugo Larochelle, and Daniel Tarlow. Learning graph structure with a finite-state automaton layer. *arXiv preprint arXiv:2007.04929*, 2020.
- [26] Seyed Mehran Kazemi, Rishab Goel, Kshitij Jain, Ivan Kobyzev, Akshay Sethi, Peter Forsyth, and Pascal Poupart. Representation learning for dynamic graphs: A survey. *JMLR*, 2020.
- [27] Anees Kazi, Luca Cosmo, Nassir Navab, and Michael Bronstein. Differentiable graph module (dgm) for graph convolutional networks. *arXiv preprint arXiv:2002.04999*, 2020.
- [28] Diederik P Kingma and Jimmy Ba. Adam: A method for stochastic optimization. *arXiv preprint arXiv:1412.6980*, 2014.
- [29] Thomas N. Kipf and Max Welling. Semi-supervised classification with graph convolutional networks. In *ICLR*, 2017.
- [30] Nikita Kitaev, Łukasz Kaiser, and Anselm Levskaya. Reformer: The efficient transformer. *arXiv preprint arXiv:2001.04451*, 2020.
- [31] Yann LeCun, Corinna Cortes, and CJ Burges. Mnist handwritten digit database. *ATT Labs [Online]*. Available: <http://yann.lecun.com/exdb/mnist>, 2, 2010.
- [32] Guohao Li, Matthias Muller, Ali Thabet, and Bernard Ghanem. Deepgcns: Can gcns go as deep as cnns? In *Proceedings of the IEEE/CVF International Conference on Computer Vision*, pages 9267–9276, 2019.
- [33] Qimai Li, Zhichao Han, and Xiao-Ming Wu. Deeper insights into graph convolutional networks for semi-supervised learning. In *AAAI*, 2018.
- [34] Ruoyu Li, Sheng Wang, Feiyun Zhu, and Junzhou Huang. Adaptive graph convolutional neural networks. *arXiv preprint arXiv:1801.03226*, 2018.
- [35] Renjie Liao, Yujia Li, Yang Song, Shenlong Wang, Charlie Nash, William L Hamilton, David Duvenaud, Raquel Urtasun, and Richard S Zemel. Efficient graph generation with graph recurrent attention networks. *arXiv preprint arXiv:1910.00760*, 2019.
- [36] Jenny Liu, Aviral Kumar, Jimmy Ba, Jamie Kiros, and Kevin Swersky. Graph normalizing flows. In *NeurIPS*, pages 13556–13566, 2019.
- [37] Wei Liu, Junfeng He, and Shih-Fu Chang. Large graph construction for scalable semi-supervised learning. In *ICML*, 2010.

- [38] Vinod Nair and Geoffrey E Hinton. Rectified linear units improve restricted boltzmann machines. In *Icml*, 2010.
- [39] Kenta Oono and Taiji Suzuki. Graph neural networks exponentially lose expressive power for node classification. In *ICLR*, 2020.
- [40] Adam Paszke, Sam Gross, Soumith Chintala, Gregory Chanan, Edward Yang, Zachary DeVito, Zeming Lin, Alban Desmaison, Luca Antiga, and Adam Lerer. Automatic differentiation in pytorch. In *NIPS-W*, 2017.
- [41] Fabian Pedregosa, Gaël Varoquaux, Alexandre Gramfort, Vincent Michel, Bertrand Thirion, Olivier Grisel, Mathieu Blondel, Peter Prettenhofer, Ron Weiss, Vincent Dubourg, et al. Scikit-learn: Machine learning in python. *JMLR*, 12:2825–2830, 2011.
- [42] Bryan Perozzi, Rami Al-Rfou, and Steven Skiena. Deepwalk: Online learning of social representations. In *Proceedings of the 20th ACM SIGKDD international conference on Knowledge discovery and data mining*, pages 701–710, 2014.
- [43] Shah Rukh Qasim, Jan Kieseler, Yutaro Iiyama, and Maurizio Pierini. Learning representations of irregular particle-detector geometry with distance-weighted graph networks. *The European Physical Journal C*, 79(7):1–11, 2019.
- [44] Sam T Roweis and Lawrence K Saul. Nonlinear dimensionality reduction by locally linear embedding. *science*, 290(5500):2323–2326, 2000.
- [45] Franco Scarselli, Marco Gori, Ah Chung Tsoi, Markus Hagenbuchner, and Gabriele Monfardini. The graph neural network model. *IEEE Transactions on Neural Networks*, 20(1):61–80, 2008.
- [46] Prithviraj Sen, Galileo Namata, Mustafa Bilgic, Lise Getoor, Brian Galligher, and Tina Eliassi-Rad. Collective classification in network data. *AI magazine*, 29(3):93–93, 2008.
- [47] Otilia Stretcu, Krishnamurthy Viswanathan, Dana Movshovitz-Attias, Emmanouil Platanios, Sujith Ravi, and Andrew Tomkins. Graph agreement models for semi-supervised learning. In *NeurIPS*, pages 8713–8723, 2019.
- [48] Mohammed Suhail and Leonid Sigal. Mixture-kernel graph attention network for situation recognition. In *Proceedings of the IEEE International Conference on Computer Vision*, pages 10363–10372, 2019.
- [49] Joshua B Tenenbaum, Vin De Silva, and John C Langford. A global geometric framework for nonlinear dimensionality reduction. *science*, 290(5500):2319–2323, 2000.
- [50] Petar Veličković, Guillem Cucurull, Arantxa Casanova, Adriana Romero, Pietro Lio, and Yoshua Bengio. Graph attention networks. In *ICLR*, 2018.
- [51] Pascal Vincent, Hugo Larochelle, Yoshua Bengio, and Pierre-Antoine Manzagol. Extracting and composing robust features with denoising autoencoders. In *ICML*, pages 1096–1103, 2008.
- [52] Minjie Wang, Lingfan Yu, Da Zheng, Quan Gan, Yu Gai, Zihao Ye, Mufei Li, Jinjing Zhou, Qi Huang, Chao Ma, et al. Deep graph library: Towards efficient and scalable deep learning on graphs. *arXiv preprint arXiv:1909.01315*, 2019.
- [53] Yue Wang, Yongbin Sun, Ziwei Liu, Sanjay E Sarma, Michael M Bronstein, and Justin M Solomon. Dynamic graph cnn for learning on point clouds. *Acm Transactions On Graphics (tog)*, 38(5):1–12, 2019.
- [54] Xuan Wu, Lingxiao Zhao, and Leman Akoglu. A quest for structure: Jointly learning the graph structure and semi-supervised classification. In *CIKM*, pages 87–96, 2018.
- [55] Liang Yang, Zesheng Kang, Xiaochun Cao, Di Jin, Bo Yang, and Yuanfang Guo. Topology optimization based graph convolutional network. In *IJCAI*, pages 4054–4061, 2019.
- [56] Jiaxuan You, Rex Ying, Xiang Ren, William L Hamilton, and Jure Leskovec. Graphrnn: Generating realistic graphs with deep auto-regressive models. *arXiv preprint arXiv:1802.08773*, 2018.

- [57] Yuning You, Tianlong Chen, Zhangyang Wang, and Yang Shen. When does self-supervision help graph convolutional networks? *arXiv preprint arXiv:2006.09136*, 2020.
- [58] Donghan Yu, Ruohong Zhang, Zhengbao Jiang, Yuexin Wu, and Yiming Yang. Graph-revised convolutional network. In *ECML PKDD*, 2020.
- [59] Jiani Zhang, Xingjian Shi, Junyuan Xie, Hao Ma, Irwin King, and Dit-Yan Yeung. Gaan: Gated attention networks for learning on large and spatiotemporal graphs. *arXiv preprint arXiv:1803.07294*, 2018.
- [60] Jiawei Zhang, Haopeng Zhang, Congying Xia, and Li Sun. Graph-bert: Only attention is needed for learning graph representations. *arXiv preprint arXiv:2001.05140*, 2020.
- [61] Tong Zhao, Yozen Liu, Leonardo Neves, Oliver Woodford, Meng Jiang, and Neil Shah. Data augmentation for graph neural networks. *arXiv preprint arXiv:2006.06830*, 2020.
- [62] Hao Zhu, Yankai Lin, Zhiyuan Liu, Jie Fu, Tat-seng Chua, and Maosong Sun. Graph neural networks with generated parameters for relation extraction. *arXiv preprint arXiv:1902.00756*, 2019.
- [63] Jiong Zhu, Yujun Yan, Lingxiao Zhao, Mark Heimann, Leman Akoglu, and Danai Koutra. Beyond homophily in graph neural networks: Current limitations and effective designs. *Advances in Neural Information Processing Systems*, 33, 2020.
- [64] Qikui Zhu, Bo Du, and Pingkun Yan. Self-supervised training of graph convolutional networks. *arXiv preprint arXiv:2006.02380*, 2020.
- [65] Xiaojin Zhu and Zoubin Ghahramani. Learning from labeled and unlabeled data with label propagation. 2002.
- [66] Xiaojin Zhu, Zoubin Ghahramani, and John D Lafferty. Semi-supervised learning using gaussian fields and harmonic functions. In *Proceedings of the 20th International conference on Machine learning (ICML-03)*, pages 912–919, 2003.
- [67] Yanqiao Zhu, Weizhi Xu, Jinghao Zhang, Qiang Liu, Shu Wu, and Liang Wang. Deep graph structure learning for robust representations: A survey. *arXiv preprint arXiv:2103.03036*, 2021.
- [68] Daniel Zügner, Amir Akbarnejad, and Stephan Günnemann. Adversarial attacks on neural networks for graph data. In *Proceedings of the 24th ACM SIGKDD International Conference on Knowledge Discovery & Data Mining*, pages 2847–2856, 2018.

A More Experiments and Analyses

Importance of k in kNN: Figure 7 shows the performance of SLAPS on Cora for three graph generators as a function of k in kNN. For all three cases, the value of k plays a major role in model performance. The FP generator is the least sensitive because, in FP, k only affects the initialization of the adjacency matrix but then the model can change the number of neighbors of each node. For MLP and MLP-D, however, the number of neighbors of each node remains close to k (but not necessarily equal as the adjacency processor can add or remove some edges) and the two generators become more sensitive to k . For larger values of k , the extra flexibility of the MLP generator enables removing some of the unwanted edges through the function P or reducing the weights of the unwanted edges resulting in MLP being less sensitive to large values of k compared to MLP-D.

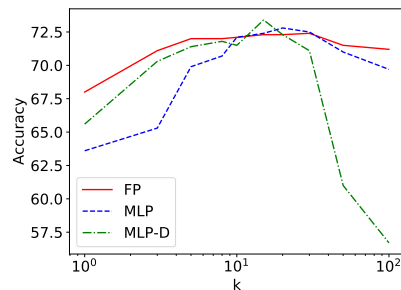


Figure 7: The performance of SLAPS on Cora as a function of k in kNN.

Increasing the number of layers: In the main text, we described how some edges may receive no supervision during latent graph learning. We pointed out that while increasing the number of

layers of the GCN may alleviate the problem to some extent, deeper GCNs typically provide inferior results due to issues such as oversmoothing [see, e.g., 33, 39]. We empirically tested deeper GCNs for latent graph learning to see if simply using more layers can obviate the need for the proposed self-supervision. Specifically, we tested SLAPS without self-supervision (i.e. $\lambda = 0$) with 2, 4, and 6 layers on Cora. We also added residual connections that have been shown to help train deeper GCNs [32]. The accuracies for 2, 4, and 6-layer models are 66.2%, 67.1%, and 55.8% respectively. It can be viewed that increasing the number of layers from 2 to 4 provides an improvement. This might be because the benefit provided by a 4-layer model in terms of alleviating the starved edge problem outweighs the increase in oversmoothing. However, when the number of layers increases to 6, the oversmoothing problem outweighs and the performance drops significantly. Further increasing the number of layers resulted in even lower accuracies.

Symmetrization: In the adjacency processor, we used the following equation:

$$\mathbf{A} = \mathbf{D}^{-\frac{1}{2}} \left(\frac{\mathbf{P}(\tilde{\mathbf{A}}) + \mathbf{P}(\tilde{\mathbf{A}})^T}{2} \right) \mathbf{D}^{-\frac{1}{2}}$$

which symmetrized the adjacency matrix by taking the average of $\mathbf{P}(\tilde{\mathbf{A}})$ and $\mathbf{P}(\tilde{\mathbf{A}})^T$. Here we also consider two other choices: 1) $\max(\mathbf{P}(\tilde{\mathbf{A}}), \mathbf{P}(\tilde{\mathbf{A}})^T)$, and 2) not symmetrizing the adjacency (i.e. using $\mathbf{P}(\tilde{\mathbf{A}})$). Figure 8 compares these three choices on Cora and Citeseer with an MLP generator (other generators produced similar results). On both datasets, symmetrizing the adjacency provides a performance boost. Compared to mean symmetrization, max symmetrization performs slightly worse. This may be because max symmetrization does not distinguish between the case where both v_i and v_j are among the k most similar nodes of each other and the case where only one of them is among the k most similar nodes of the other.

Fixing a prior graph manually instead of using self-supervision: In the main text, we validated Hypothesis 1 by adding a self-supervised task to encourage learning a graph structure that is appropriate for predicting the node features, and showing in our experiments how this additional task helps improve the results. Here, we provide more evidence for the validity of Hypothesis 1 by showing that we can obtain good results even when regularizing the learned graph structure toward a manually fixed structure that is appropriate for predicting the node features.

Toward this goal, we experimented with Cora and Citeseer and created a cosine similarity graph as our prior graph \mathbf{A}^{prior} where the edge weights correspond to the cosine similarity of the nodes. We sparsified \mathbf{A}^{prior} by connecting each node only to the k most similar nodes. Then, we added a term $\lambda \|\mathbf{A} - \mathbf{A}^{prior}\|_F$ to the loss function where λ is a hyperparameter, \mathbf{A} is the learned graph structure (i.e. the output of the graph generator), and $\|\cdot\|_F$ shows the Frobenius norm. Note that \mathbf{A}^{prior} exhibits homophily with respect to the node features because the node features in Cora and Citeseer are binary, so two nodes that share the same values for more features have a higher similarity and are more likely to be connected.

The results can be viewed in Figure 9. According to the results, we can see that regularizing toward a manually designed \mathbf{A}^{prior} also provides good results but falls short of SLAPS with self-supervision. The superiority of the self-supervised approach compared to the manual design could be due to two reasons.

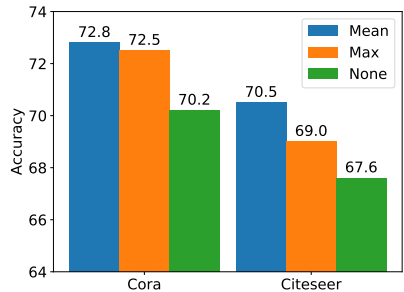


Figure 8: The performance of SLAPS on Cora and Citeseer with different adjacency symmetrizations.

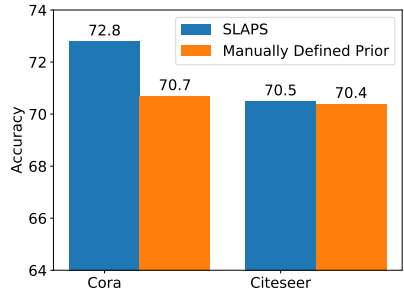


Figure 9: The performance of SLAPS and regularization toward a manually defined prior structure on Cora and Citeseer when using the MLP generator.

- Some of the node features may be redundant (e.g., they may be derived from other features) or highly correlated. These features can negatively affect the similarity computations for the prior graph in A^{prior} . As an example, consider three nodes with seven binary features $[0, 0, 0, 1, 1, 1, 1]$, $[0, 0, 0, 0, 0, 0, 0]$ and $[1, 1, 1, 1, 1, 1, 1]$ respectively and assume the last two features for each node are always equivalent and are computed based on a *logical and* of the 4th and 5th features⁵. Without these two features, the first node is more similar to the second than the third node, but when considering these derived features, it becomes more similar to the third node. This change in node similarities affects the construction of A^{prior} which can deteriorate the overall performance of the model. The version of SLAPS with the self-supervised task, on the other hand, is not affected by this problem as much because the model can learn to predict the derived node features based on other features and without heavily relying on the graph structure.
- While many graph structures may be appropriate for predicting the node features, in the manual approach we only regularize toward one particular such structure. Using the self-supervised task, however, SLAPS can learn any of those structures; ideally, it learns the one that is more suited for the downstream task due to the extra supervision coming from the downstream task.

B Implementation Details

We implemented our model in PyTorch [40], used deep graph library (DGL) [52] for the sparse operations, and used Adam [28] as the optimizer. We performed early stopping and hyperparameter tuning based on the accuracy on the validation set for all datasets except Wine and Cancer. For these two datasets, the validation accuracy reached 100 percent with many hyperparameter settings, making it difficult to select the best set of hyperparameters. Instead, we used the validation cross-entropy loss for these two datasets.

We fixed the maximum number of epochs to 2000. We use two-layer GCNs for both GNN_C and GNN_{DAE} as well as for baselines and two-layer MLPs throughout the paper (for experiments on ogbn-arxiv, although the original paper uses models with three layers and with batch normalization after each layer, to be consistent with our other experiments we used two layers and removed the normalization). We used two learning rates, one for GNN_C as lr_C and one for the other parameters of the models as lr_{DAE} . We tuned the two learning rates from the set $\{0.01, 0.001\}$. We added dropout layers with dropout probabilities of 0.5 after the first layer of the GNNs. We also added dropout to the adjacency matrix for both GNN_C and GNN_{DAE} as $dropout_C$ $dropout_{DAE}$ respectively and tuned the values from the set $\{0.25, 0.5\}$. We set the hidden dimension of GNN_C to 32 for all datasets except for ogbn-arxiv for which we set it to 256. We used cosine similarity for building the kNN graphs and tuned the value of k from the set $\{10, 15, 20, 30\}$. We tuned λ (λ controls the relative importance of the two losses) from the set $\{0.1, 1, 10, 100, 500\}$. We tuned r and η from the sets $\{1, 5, 10\}$ and $\{1, 5\}$ respectively. The best set of hyperparameters for each dataset chosen on the validation set is in table 4. The code of our experiments will be available upon acceptance of the paper.

For GRCN [58], DGCNN [53], and IDGL [6], we used the code released by the authors and tuned the hyperparameters as suggested in the original papers. The results of LDS [13] are directly taken from the original paper. For LP [66], we used scikit-learn python package [41].

All the results for our model and the baselines are averaged over 10 runs. We report the mean and standard deviation. We ran all the experiments on a single GPU (NVIDIA GeForce GTX 1080 Ti).

Self-training and AdaEdge: We combined SLAPS (and kNN-GCN) with two techniques from the literature namely *self-training* and *AdaEdge*. For completeness sake, we provide a brief description of these approaches and refer the reader to the original papers for detailed descriptions.

For self-training, we first trained a model using the existing labels in the training set. Then we used this model to make predictions for the unlabeled nodes that were not in the train, validation, or test sets. We considered the label predictions for the top ζ most confident unlabeled nodes as ground truth labels and added them to the training labels. Finally, we trained a model from scratch on the expanded set of labels. Here, ζ is a hyperparameter. We tuned its value from the set $\{50, 100, 200, 300, 400, 500\}$.

⁵For the first node in the example, the 4th and 5th features are both 1 so their logical and is also 1 and so the last two features for this node are both 1. The computation for the other two nodes is similar.

For AdaEdge, in the case of kNN-GCN, we first trained a kNN-GCN model. Then we changed the structure of the graph from the kNN graph to a new graph by following these steps: 1) add edges between nodes with the same class predictions if both prediction confidences surpass a threshold, 2) remove edge between nodes with different class predictions if both prediction confidences surpass a threshold. Then, we trained a GCN model on the new structure and repeated the aforementioned steps to generate a new structure. We did this iteratively until generating a new structure did not provide a boost in performance on the validation set. For SLAPS, we followed a similar approach except that the initial model was a SLAPS model instead of a kNN-GCN model.

kNN Implementation: For our MLP generator, we used a kNN operation to sparsify the generated graph. Here, we explain how we implemented the kNN operation to avoid blocking the gradient flow. Let $M \in \mathbb{R}^{n \times n}$ with $M_{ij} = 1$ if v_j is among the top k similar nodes to v_i and 0 otherwise, and let $S \in \mathbb{R}^{n \times n}$ with $S_{ij} = \text{Sim}(X'_i, X'_j)$ for some differentiable similarity function Sim (we used cosine). Then $\tilde{A} = \text{kNN}(X') = M \odot S$ where \odot represents the Hadamard (element-wise) product. With this formulation, in the forward phase of the network, one can first compute the matrix M using an off-the-shelf k-nearest neighbors algorithm and then compute the similarities in S only for pairs of nodes where $M_{ij} = 1$. In our experiments, we compute exact k-nearest neighbors; one can approximate it using locality-sensitive hashing approaches for larger graphs (see, e.g., [16, 30]). In the backward phase of our model, we compute the gradients only with respect to those elements in S whose corresponding value in M is 1 (i.e. those elements S_{ij} such that $M_{ij} = 1$); the gradient with respect to the other elements is 0. Since S is computed based on X' , the gradients flow to the elements in X' (and consequently to the weights of the MLP) through S .

Adjacency processor: We used a function P in our adjacency processor to make the values of the \tilde{A} positive. In our experiments, when using an MLP generator, we let P be the ReLU function applied element-wise on the elements of \tilde{A} . When using the fully-parameterized (FP) generator, applying ReLU results in a gradient flow problem as any edge whose corresponding value in \tilde{A} becomes less than or equal to zero stops receiving gradient updates. For this reason, for FP we apply the ELU [8] function to the elements of \tilde{A} and then add a value of 1.

C Dataset statistics

The statistics of the datasets used in the experiments can be found in Table 5.

D Supervision starvation in Erdős-Rényi and scale-free networks

We start by defining some new notation that helps simplify the proofs and analysis in this section. We let l_v be a random variable indicating that v is a labeled node, with \bar{l}_v indicating that its negation, $c_{v,u}$ be a random variable indicating that v is connected to u with an edge, with $\bar{c}_{v,u}$ indicating its negation, and cl_v be random variable indicating that v is connected to at least one labeled node with \bar{cl}_v indicating its negation (i.e. it indicates that v is connected to no labeled nodes).

Theorem 2 *Let $\mathcal{G}(n, m)$ be an Erdős-Rényi graph with n nodes and m edges. Assume we have labels for q nodes selected uniformly at random. The probability of an edge being a starved edge with a two-layer GCN is equal to $(1 - \frac{q}{n})(1 - \frac{q-1}{n-1}) \prod_{i=1}^{2q} (1 - \frac{m-1}{\binom{n}{2}-i})$.*

Proof 1 *To compute the probability of an edge being a starved edge, we first compute the probability of the two nodes of the edge being unlabeled themselves and then the probability of the two nodes not being connected to any labeled nodes. Let v and u represent two nodes connected by an edge.*

With n nodes and q labels, the probability of a node being labeled is $\frac{q}{n}$. Therefore, $Pr(\bar{l}_v) = (1 - \frac{q}{n})$ and $Pr(\bar{l}_u | \bar{l}_v) = (1 - \frac{q}{n-1})$. Therefore, $Pr(\bar{l}_v \wedge \bar{l}_u) = (1 - \frac{q}{n})(1 - \frac{q}{n-1})$.

Since there is an edge between v and u , there are $m - 1$ edges remaining. Also, there are $\binom{n}{2} - 1$ pairs of nodes that can potentially have an edge between them. Therefore, the probability of v being disconnected from the first labeled node is $1 - \frac{m-1}{\binom{n}{2}-1}$. If v is disconnected from the first labeled node, there are still $m - 1$ edges remaining and there are now $\binom{n}{2} - 2$ pairs of nodes that can potentially

Table 4: Best set of hyperparameters for different datasets chosen on validation set.

Dataset	Generator	lr_C	lr_{DAE}	$dropout_c$	$dropout_{DAE}$	k	λ	r	η
Cora	FP	0.001	0.01	0.5	0.25	30	10	10	5
Cora	MLP	0.01	0.001	0.25	0.5	20	10	10	5
Cora	MLP-D	0.01	0.001	0.25	0.5	15	10	10	5
Citeseer	FP	0.01	0.01	0.5	0.5	30	1	10	1
Citeseer	MLP	0.01	0.001	0.25	0.5	30	10	10	5
Citeseer	MLP-D	0.001	0.01	0.5	0.5	20	10	10	5
Cora390	FP	0.01	0.01	0.25	0.5	20	100	10	5
Cora390	MLP	0.01	0.001	0.25	0.5	20	10	10	5
Cora390	MLP-D	0.001	0.001	0.25	0.5	20	10	10	5
Citeseer370	FP	0.01	0.01	0.5	0.5	30	1	10	1
Citeseer370	MLP	0.01	0.001	0.25	0.5	30	10	10	5
Citeseer370	MLP-D	0.01	0.01	0.25	0.5	20	10	10	5
Pubmed	MLP	0.01	0.01	0.5	0.5	15	10	10	5
Pubmed	MLP-D	0.01	0.01	0.25	0.25	15	100	5	5
ogbn-arxiv	MLP	0.01	0.001	0.25	0.5	15	10	1	5
ogbn-arxiv	MLP-D	0.01	0.001	0.5	0.25	15	10	1	5
Wine	FP	0.01	0.001	0.5	0.5	20	0.1	5	5
Wine	MLP	0.01	0.001	0.5	0.25	20	0.1	5	5
Wine	MLP-D	0.01	0.01	0.25	0.5	10	1	5	5
Cancer	FP	0.01	0.001	0.5	0.25	20	0.1	5	5
Cancer	MLP	0.01	0.001	0.5	0.5	20	1.0	5	5
Cancer	MLP-D	0.01	0.01	0.5	0.5	20	0.1	5	5
Digits	FP	0.01	0.001	0.25	0.5	20	0.1	5	5
Digits	MLP	0.01	0.001	0.25	0.5	20	10	5	5
Digits	MLP-D	0.01	0.001	0.5	0.25	15	0.1	5	5
20news	FP	0.01	0.01	0.5	0.5	20	500	5	5
20news	MLP	0.001	0.001	0.25	0.5	20	500	5	5
20news	MLP-D	0.01	0.01	0.25	0.25	20	100	5	5
MNIST (1000)	MLP	0.01	0.01	0.5	0.5	15	10	10	5
MNIST (2000)	MLP-D	0.01	0.001	0.5	0.5	15	100	10	5
MNIST (3000)	MLP	0.01	0.01	0.5	0.5	15	10	5	5

have an edge between them. So the probability of v being disconnected from the second node given that it is disconnected from the first labeled node is $1 - \frac{m-1}{\binom{n}{2}-2}$. With similar reasoning, we can see that the probability of v being disconnected from the i -th labeled node given that it is disconnected from the first $i - 1$ labeled nodes is $1 - \frac{m-1}{\binom{n}{2}-i}$.

We can follow similar reasoning for u . The probability of u being disconnected from the first labeled node given that v is disconnected from all q labeled nodes is $1 - \frac{m-1}{\binom{n}{2}-q-1}$. That is because there are still $m - 1$ edges remaining and $\binom{n}{2} - q - 1$ pairs of nodes that can potentially be connected with an edge. We can also see that the probability of u being disconnected from the i -th labeled node given that it is disconnected from the first $i - 1$ labeled nodes and that v is disconnected from all q labeled nodes is $1 - \frac{m-1}{\binom{n}{2}-q-i}$.

As the probability of the two nodes being unlabeled and not being connected to any labeled nodes in the graph are independent, their joint probability is the multiplication of their probabilities computed above and it is equal to $(1 - \frac{q}{n})(1 - \frac{q}{n-1}) \prod_{i=1}^{2q} (1 - \frac{m-1}{\binom{n}{2}-i})$.

Barabási–Albert and scale-free networks: We also extend the above result for Erdős–Rényi graphs to the Barabási–Albert [2] model. Since Barabási–Albert graph generation results in scale-free networks with a scale parameter $\gamma = -3$, we present results for the general case of scale-free networks as it makes the analysis simpler and more general. In what follows, we compute the probability of an edge being a starved edge in a scale-free network.

Table 5: Dataset statistics.

Dataset	Nodes	Edges	Classes	Features	Label rate
Cora	2,708	5,429	7	1,433	0.052
Citeseer	3,327	4,732	6	3,703	0.036
Pubmed	19,717	44,338	3	500	0.003
ogbn-arxiv	169,343	1,166,243	40	128	0.537
Wine	178	0	3	13	0.112
Cancer	569	0	2	30	0.035
Digits	1,797	0	10	64	0.056
20news	9,607	0	10	236	0.021
MNIST	10,000	0	10	784	0.1, 0.2 and 0.3

Let \mathcal{G} be a scale-free network with n nodes, q labels (selected uniformly at random), and scale parameter γ . Then, if we select a random edge between two nodes v and u , the probability of the edge between them being a starved edge is:

$$Pr(\bar{l}_v) * Pr(\bar{l}_u|\bar{l}_v) * Pr(\bar{c}l_v|c_{v,u}, \bar{l}_v, \bar{l}_u) * Pr(\bar{c}l_u|c_{v,u}, \bar{l}_v, \bar{l}_u, \bar{c}l_v).$$

Each of these terms can be computed as follows ($\binom{a}{b}$ represents the number of combinations of selecting b items from a set with a items):

- $Pr(\bar{l}_v) = (1 - \frac{q}{n})$
- $Pr(\bar{l}_u|\bar{l}_v) = (1 - \frac{q}{n-1})$
- $Pr(\bar{c}l_v|c_{v,u}, \bar{l}_v, \bar{l}_u) = \frac{\sum_{k=1}^{n-1} k^\gamma \binom{n-q-2}{k-1}}{\sum_{k=1}^{n-1} k^\gamma \binom{n-2}{k-1}}$

For a large enough network, $Pr(\bar{c}l_u|c_{v,u}, \bar{l}_v, \bar{l}_u, \bar{c}l_v)$ can be approximated as $Pr(\bar{c}l_u|c_{v,u}, \bar{l}_v, \bar{l}_u)$ and it can be computed similarly as the previous case.

With the derivation above, for a scale-free network with $n = 2708$ and $q = 140$ (corresponding to the stats from Cora), the probability of an edge being a starved edge for $\gamma = -3$ is 0.87 and for $\gamma = -2$ is 0.76 .

E Why not compare the learned graph structures with the original ones?

A comparison between the learned graph structures using SLAPS (or other baselines) and the original graph structure of the datasets we used may not be sensible. We explain this using an example. Before getting into the example, we remind the reader that the goal of structure learning for semi-supervised classification with graph neural networks is to learn a structure with a high degree of homophily. Following [63], we define the *edge homophily ratio* as the fraction of edges in the graph that connect nodes that have the same class label.

Figure 10 demonstrates an example where two graph structures for the same set of nodes have the same edge homophily ratio (0.8 for both) but have no edges in common. For our task, it is possible that the original graph structure (e.g., the citation graph in Cora) corresponds to the structure on the left but SLAPS (or any other model) learns the graph on the right, or vice versa. While both these structures may be equally good⁶, they do not share any edges. Therefore, measuring the quality of the learned graph using SLAPS by comparing it to the original graph of the datasets may not be sensible. However, if a noisy version of the initial structure is provided as input for SLAPS, then one may expect that SLAPS recovers a structure similar to the cleaned original graph and this is indeed what we demonstrate in the main text.

⁶We are disregarding the features for simplicity sake.

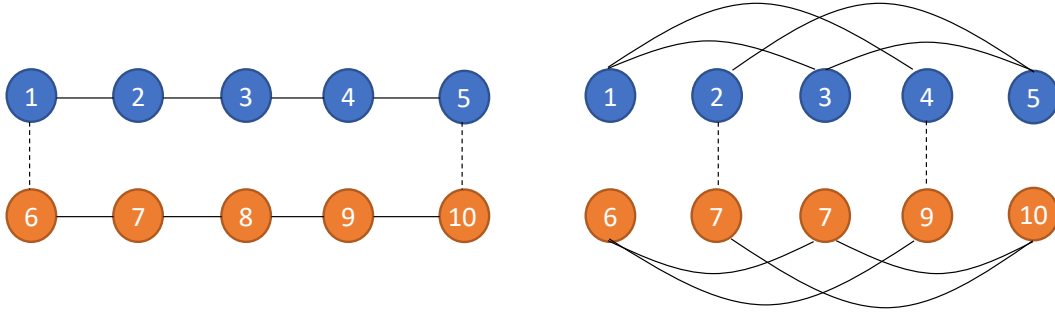


Figure 10: Two example graph structures. Node colors indicates the class labels. Solid lines indicate homophilous edges and dashed lines indicate non-homophilous edges. The two graphs exhibit the same degree of homophily yet there is not overlap between their edges.

F Limitations

In this section, we discuss some of the limitations of the proposed model. Firstly, in cases where nodes do not have input features but an initial noisy structure of the nodes is available, our self-supervised task cannot be readily applied. One possible solution is to first run an unsupervised node embedding model such as DeepWalk [42] to obtain node embeddings, then treat these embeddings as node features and run SLAPS. Secondly, the FP graph generator is not applicable in the inductive setting; this is because FP directly optimizes the adjacency matrix. However, our other two graph generators (MLP and MLP-D) can be applied in the inductive setting.